

Flux rectification in the quantum XXZ chain

Gabriel T. Landi* and E. Novais

Universidade Federal do ABC, 09210-580 Santo André, Brazil

Mário J. de Oliveira

Instituto de Física, Universidade de São Paulo, 05314-970 São Paulo, Brazil

Dragi Karevski

*Université de Lorraine, Institut Jean Lamour, Vandoeuvre lès Nancy F-54506, France
and CNRS, UMR 7198, IJL, Groupe de Physique Statistique, Nancy, France*

(Received 10 July 2014; revised manuscript received 9 October 2014; published 30 October 2014)

Thermal rectification is the phenomenon by which the flux of heat depends on the direction of the flow. It has attracted much interest in recent years due to the possibility of devising thermal diodes. In this paper, we consider the rectification phenomenon in the quantum XXZ chain subject to an inhomogeneous field. The chain is driven out of equilibrium by the contact at its boundaries with two different reservoirs, leading to a constant flow of magnetization from one bath to the other. The nonunitary dynamics of this system, which is modeled by a Lindblad master equation, is treated exactly for small sizes and numerically for larger ones. The functional dependence of the rectification coefficient on the model parameters (anisotropy, field amplitude, and out of equilibrium driving strength) is investigated in full detail. Close to the XX point and at small inhomogeneity and low driving, we have found an explicit expression for the rectification coefficient that is valid at all system sizes. In particular, it shows that the phenomenon of rectification persists even in the thermodynamic limit. Finally, we prove that in the case of the XX chain, there is no rectification.

DOI: [10.1103/PhysRevE.90.042142](https://doi.org/10.1103/PhysRevE.90.042142)

PACS number(s): 05.50.+q, 44.10.+i, 71.10.-w

I. INTRODUCTION

When a system is placed in contact with two heat reservoirs maintained at a temperature difference ΔT , it eventually reaches a nonequilibrium steady state (NESS) characterized by a constant heat flux J from the hotter to the colder reservoir. If we reverse the baths by making $\Delta T \rightarrow -\Delta T$, and if the system is symmetric, we expect that $J(-\Delta T) = -J(\Delta T)$; that is, the flux should simply change direction. Conversely, if the system is asymmetric, it is possible that $J(-\Delta T) \neq -J(\Delta T)$. In this case, we say the system presents *thermal rectification*, a name given in analogy to the electric rectification of diodes.

Thermal rectification was first observed by Starr [1,2] in 1936 and, after many years of dormancy, has gained renewed interest in recent years, both experimentally [3–8] and theoretically [9–12]. Much of this interest derives from the possibility of developing thermal integrated circuits which operate on heat instead of electric currents. The concept of a thermal diode was put forth by Li *et al.* [13] and subsequently demonstrated experimentally by Chang *et al.* [8] using nanotubes. In the following years, the concepts of thermal logic gates [14] and thermal transistors [15] have also been proposed. For recent reviews, see [16,17].

Besides the applied interest, this phenomenon also raises some fundamental questions. In particular, one may inquire about the necessary ingredients for the existence of rectification. Clearly, the system must be asymmetric. This, however, does not necessarily suffice. As discussed by Pereira [18], in

graded classical systems, the rectification is identically zero if the interactions are harmonic. A good example is the classical harmonic chain of Rieder *et al.* [19], where the system is modeled by a chain of particles connected by harmonic springs, with the first and last particles connected to heat baths via a Langevin equation. In this system, it can be shown that, irrespective of the nature of the asymmetry, the flux J is always an odd function of ΔT .

The need for introducing asymmetries and more complex interactions makes any analytical treatment of this problem much more difficult. In fact, we are unaware of any papers in the literature which deal with rectification exactly. Part of the purpose of this paper is to fill this gap. Our goal is to study rectification in a model that can be approached analytically. With this in mind, we then discuss what the necessary ingredients are for the existence of rectification and also some of its general properties. This, we hope, will give further insight into this scientifically interesting and technologically important problem.

The system under study is the open one-dimensional quantum XXZ chain subject to two baths at each end. The dynamics is modeled by a Lindblad master equation [20–24] and the asymmetry needed to generate a rectifying behavior is introduced by means of an inhomogeneous magnetic field acting on each site of the chain. For the homogeneous XXZ chain, it has been shown for a specific pair of Lindblad boundary terms that the exact stationary density matrix is given explicitly as a matrix product state involving the infinite representation of the quantum algebra $U_q[\text{SU}(2)]$ [21,23]. Using the explicit steady-state density matrix, exact magnetization profiles and magnetization currents have been computed for the isotropic XXX chain with N sites [25]. In particular, it has been shown that for twisted boundary conditions, the

*gtlandi@gmail.com

longitudinal and transverse magnetization currents behave qualitatively differently with the system size N [25].

We begin by describing the model in detail in Sec. II. Some general properties of the rectification are discussed in Sec. III and the method of solution we employed is explained in Sec. IV. Afterwards we present the solution for a chain of $N = 2$ and 3 spins in Secs. V and VI. This is followed with the numerical solution for larger system sizes presented in Sec. VII. Here we obtain a particularly interesting result: by combining our exact calculations with the numerical solutions, we are able to access the behavior of the rectification for any size. We then use this to show that in the thermodynamic limit, the rectification remains finite. Finally, in Sec. VIII we prove that in the XX chain, the rectification is always zero. The importance of this result lies in the resemblance to the aforementioned fact that the rectification is zero in a classical harmonic chain. Indeed, when written in terms of fermionic creation and annihilation operators, the XX chain contains only quadratic terms, whereas in the XXZ chain, a quartic term appears.

II. DESCRIPTION OF THE MODEL

We consider a one-dimensional spin chain with N sites, each described by Pauli matrices σ_i^x , σ_i^y , and σ_i^z . The Hamiltonian is chosen to be of the XXZ form,

$$H = \sum_{i=1}^N h_i \sigma_i^z + \sum_{i=1}^{N-1} \{ \alpha (\sigma_i^x \sigma_{i+1}^x + \sigma_i^y \sigma_{i+1}^y) + \Delta \sigma_i^z \sigma_{i+1}^z \}, \quad (1)$$

where h_i is the magnetic field acting on site i and, throughout, we will usually set $\alpha = 1$.

This spin chain is coupled to two baths at each end. Assuming the Born-Markov approximation, we may describe the time evolution of the density matrix ρ of the system using the Lindblad master equation [20]:

$$\frac{d\rho}{dt} = -i[H, \rho] + D_L(\rho) + D_R(\rho), \quad (2)$$

where we set $\hbar = 1$. The dissipative parts D_L and D_R of the equation are defined in terms of spin creation and annihilation operators $\sigma_i^\pm = (\sigma_i^x \pm i\sigma_i^y)/2$, as

$$D_L(\rho) = \sum_{r=\pm} 2L_r \rho L_r^\dagger - \{L_r^\dagger L_r, \rho\}, \quad (3)$$

where $L_\pm = \sqrt{\gamma(1 \pm f_L)} \sigma_1^\pm$ and $\{\cdot\}$ is the anticommutator. Similar definitions hold for D_R with σ_N^\pm and f_R instead of σ_1^\pm and f_L . The complete dissipator $D(\rho) = D_L(\rho) + D_R(\rho)$ thus reads

$$\begin{aligned} D(\rho) = & \gamma \{ (1 + f_L) [2\sigma_1^+ \rho \sigma_1^- - (\sigma_1^- \sigma_1^+ \rho + \rho \sigma_1^- \sigma_1^+)] \\ & + (1 - f_L) [2\sigma_1^- \rho \sigma_1^+ - (\sigma_1^+ \sigma_1^- \rho + \rho \sigma_1^+ \sigma_1^-)] \\ & + (1 + f_R) [2\sigma_N^+ \rho \sigma_N^- - (\sigma_N^- \sigma_N^+ \rho + \rho \sigma_N^- \sigma_N^+)] \\ & + (1 - f_R) [2\sigma_N^- \rho \sigma_N^+ - (\sigma_N^+ \sigma_N^- \rho + \rho \sigma_N^+ \sigma_N^-)] \}. \quad (4) \end{aligned}$$

The dimension of ρ is $d = 2^N$. The master equation (2) can be derived, for instance, using the repeated interactions scheme, as demonstrated in Appendices A and B. We are interested in

the steady-state solution ρ_{ss} of Eq. (2) which is obtained by setting $d\rho_{ss}/dt = 0$. We write it as

$$\mathcal{W}(\rho_{ss}) = -i[H, \rho_{ss}] + D(\rho_{ss}) = 0. \quad (5)$$

Thus, to compute the steady state, we must find the null space of the linear superoperator \mathcal{W} .

The two baths are characterized by the parameters f_L and f_R . They can be interpreted as $f_L = \langle \sigma_0^z \rangle$ and $f_R = \langle \sigma_{N+1}^z \rangle$, where the spins 0 and $N + 1$ are not a part of the chain (which runs from 1 to N ; see Appendix A). Thus, in this framework, we are fixing the average magnetization at the boundaries. When $f_L \neq f_R$, the system will evolve to a nonequilibrium steady state (NESS) characterized by a constant flow of magnetization from one bath to the other. Conversely, when $f_L = f_R$, the system relaxes to a steady state with no flux.

The flux may be found from the equation governing the time evolution of the expectation value of σ_i^z . Using Eq. (2), it can be shown that

$$\frac{d}{dt} \langle \sigma_1^z \rangle = J_L - J_1, \quad (6)$$

$$\frac{d}{dt} \langle \sigma_i^z \rangle = J_{i-1} - J_i, \quad i = 2, \dots, N-1, \quad (7)$$

$$\frac{d}{dt} \langle \sigma_N^z \rangle = J_{N-1} - J_R, \quad (8)$$

where

$$J_k = 2\alpha \langle \sigma_k^x \sigma_{k+1}^y - \sigma_k^y \sigma_{k+1}^x \rangle \quad (9)$$

is the magnetization flux from site k toward site $k + 1$, and

$$J_L = 4\gamma (f_L - \langle \sigma_1^z \rangle), \quad (10)$$

$$J_R = -4\gamma (f_R - \langle \sigma_N^z \rangle) \quad (11)$$

are the fluxes from the left bath to the system and from the system to the right bath, respectively. In the steady state $d\langle \sigma_i^z \rangle/dt = 0$, yielding a homogenous flux J through the chain,

$$J_L = J_1 = J_2 = \dots = J_N = J_R \equiv J.$$

It is worth mentioning that the system Hamiltonian (1) can be mapped into a problem of hard-core bosons (the Tonks-Girardeau model) by writing it in terms of the creation and annihilation operators σ_i^\pm [26],

$$\begin{aligned} H = & \sum_{i=1}^N h_i (2\sigma_i^+ \sigma_i^- - 1) + \sum_{i=1}^N \{ 2\alpha (\sigma_i^+ \sigma_{i+1}^- + \sigma_i^- \sigma_{i+1}^+) \\ & + \Delta [1 - 2(\sigma_i^+ \sigma_i^- - \sigma_{i+1}^+ \sigma_{i+1}^-)^2] \}. \quad (12) \end{aligned}$$

Hence, instead of interpreting J as a flux of magnetization, we may interpret it as a flux of particles in a lattice with inhomogeneous chemical potential $2h_i$. We see that the terms proportional to α give rise to a quadratic hopping term, whereas the Z term (proportional to Δ) becomes quartic in this representation and describes a two-body interaction.

III. RECTIFICATION

For simplicity, we will assume a symmetric coupling constant,

$$f_L = -f_R = f. \quad (13)$$

We may then write the steady-state flux as $J(f)$. To study the rectification, we must compare $J(f)$ with $J(-f)$, which is the flux obtained when the baths are reversed. If the system is symmetric, the flux will be an odd function of f , i.e., $J(-f) = -J(f)$. Otherwise, even though the sign of $J(-f)$ will still be opposite to that of $J(f)$, in general we will have $J(-f) \neq -J(f)$. In this situation, we say the system presents rectification. To quantify this, we define the rectification coefficient as

$$R = \frac{J(f) + J(-f)}{J(f) - J(-f)}. \quad (14)$$

It is zero when there is no rectification and has extrema ± 1 if the flux in one direction behaves as a perfect insulator. Also, by definition, $R(-f) = -R(f)$.

Alternatively, we could take the following approach: For this choice of master equation, the flux is independent of a constant shift in all the h_i . Hence we may choose the h_i to interpolate, say linearly, between $-h$ and h . This reduces the number of parameters in the system to 5: α , Δ , and h (characterizing the Hamiltonian), and f and γ (characterizing the bath). With this choice for the h_i , we may now reverse the system instead of reversing the bath. This means changing $h \rightarrow -h$. If we let $J(h)$ denote the flux for a given value of h , then we must compare $J(h)$ with $J(-h)$. Note, however, that when we reverse the system, the flux will *not* change sign. If the system presents no rectification, then $J(h) = J(-h)$. Thus, we may define the rectification coefficient as

$$R = \frac{J(h) - J(-h)}{J(h) + J(-h)}. \quad (15)$$

Note the sign difference when compared to Eq. (14). Of course, by symmetry arguments, this definition must coincide exactly with that of Eq. (14). Moreover, we again have $R(-h) = -R(h)$, so that R will be odd in both f and h .

In Sec. VIII, we shall prove the following equality:

$$J(\alpha, \Delta, h, f) = -J(\alpha, -\Delta, h, -f). \quad (16)$$

Several consequences follow from this, the most important of which is that when $\Delta = 0$,

$$J(\alpha, 0, h, f) = -J(\alpha, 0, h, -f).$$

Combining this with Eq. (14), we conclude that

$$R(\Delta = 0) = 0.$$

This fact bears a striking similarity with its classical counterpart: the term proportional to Δ in Eq. (12) is a quartic term so that, if $\Delta = 0$, our Hamiltonian becomes quadratic (harmonic). In classical systems, we also observe no rectification when the model is harmonic. Finally, it is also worth noting that Eq. (16)

implies that R will be an odd function of Δ . Hence, R is odd in h , f , and Δ .

IV. SOLUTION OF THE STEADY STATE

In this section, we describe the formal solution method employed for finding the steady-state density matrix $\rho(t \rightarrow \infty) \equiv \rho_{ss}$. Let us define $\text{vec}(A)$ as the operation of stacking the columns of a matrix A . For instance,

$$\text{vec} \begin{pmatrix} a & b \\ c & d \end{pmatrix} = \begin{pmatrix} a \\ c \\ b \\ d \end{pmatrix}.$$

For any three matrices A , B , and C , the following identity may then be directly verified:

$$\text{vec}(ABC) = (C^T \otimes A) \text{vec}(B). \quad (17)$$

Next define the vector of length $d^2 = 2^{2N}$,

$$|\rho\rangle = \text{vec}(\rho). \quad (18)$$

All operators appearing in the Lindblad master equation (2) have the form $A\rho C$. Hence we may write

$$\text{vec}(A\rho C) = (C^T \otimes A)|\rho\rangle, \quad (19)$$

$$\text{vec}(A\rho) = \text{vec}(A\rho I) = (I \otimes A)|\rho\rangle, \quad (20)$$

$$\text{vec}(\rho C) = \text{vec}(I\rho C) = (C^T \otimes I)|\rho\rangle, \quad (21)$$

where I is the identity matrix of dimension d . It is also worth noting that if we decompose the density operator as $\rho = \sum_{i,j} \rho_{ij} |i\rangle\langle j|$, on a canonical (real) orthonormal basis $\{|i\rangle\}$, then the vector representation of the density matrix is given by the tensor decomposition,

$$|\rho\rangle = \sum_{ij} \rho_{ij} |j\rangle \otimes |i\rangle. \quad (22)$$

Using these results and noting that $\text{vec}(\cdot)$ is a linear operator, we may write the master equation (2) as

$$\frac{d|\rho\rangle}{dt} = W|\rho\rangle, \quad (23)$$

where the matrix W has dimensions $d^2 = 2^{2N}$. The formal solution of this equation is

$$|\rho(t)\rangle = e^{Wt} |\rho(0)\rangle. \quad (24)$$

Let us denote by $|x_k\rangle$ and $\langle y_k|$ the right and left normalized eigenvectors ($\langle y_i|x_j\rangle = \delta_{ij}$) of W with eigenvalue λ_k ; viz,

$$W|x_k\rangle = \lambda_k|x_k\rangle, \quad (25)$$

$$\langle y_k|W = \lambda_k\langle y_k|, \quad (26)$$

where we choose to label k from 0 to $d^2 - 1$. Then,

$$W = \sum_{k=0}^{d^2-1} \lambda_k |x_k\rangle\langle y_k|. \quad (27)$$

The solution $|\rho(t)\rangle$ in Eq. (24) may thus be written as

$$|\rho(t)\rangle = \sum_{k=0}^{d^2-1} e^{\lambda_k t} |x_k\rangle \langle y_k | \rho(0)\rangle. \quad (28)$$

In the present problem, the steady-state solution of the Lindblad master equation is unique. This follows from the fact that the operators H , L_{\pm}^L , and L_{\pm}^R generate, under multiplication and addition, the entire Pauli algebra of bounded operators of the chain [27–29]. The uniqueness of the steady state means two things: (i) all the λ_k must be negative, except one (say for $k = 0$) which must be zero; (ii) the left eigenvector $\langle y_0 |$ corresponding to $\lambda_0 = 0$ must give $\langle y_k | \rho(0)\rangle = 1$ for any valid density matrix. This means

$$\langle y_0 | = \text{vec}(I)^T. \quad (29)$$

From these two properties, it then follows that the steady-state density matrix is precisely given by $|x_0\rangle$. Hence we may write Eq. (28) as

$$|\rho(t)\rangle = |\rho_{ss}\rangle + \sum_{k=1}^{d^2-1} e^{\lambda_k t} |x_k\rangle \langle y_k | \rho(0)\rangle. \quad (30)$$

Since all other λ_k have negative real parts, $|\rho(t)\rangle$ will tend to $|\rho_{ss}\rangle$ as $t \rightarrow \infty$. It is also worth noting the similarity between these results and those of the classical master equation [30].

The fact that the density matrix is given by the eigenvector $|x_0\rangle$ corresponding to $\lambda_0 = 0$ is also evident by setting $d|\rho\rangle/dt = 0$ in Eq. (23). This yields the vector analog of Eq. (5), namely,

$$W|\rho_{ss}\rangle = 0. \quad (31)$$

Or, in other words, $|\rho_{ss}\rangle$ is the vector that spans the null space of W . But the null space may be computed using Gaussian elimination, which involves only basic arithmetic operations. Hence we reach the important conclusion that $|\rho_{ss}\rangle$ (and thus J and R) will always have the form of a *ratio of polynomials* in all the parameters (no roots of high order will ever appear). This is a very interesting result since it shows that ρ_{ss} may, at least in principle, always be computed exactly. Moreover, it follows that as long as N is finite, ρ will always be analytic in all parameters (this is similar to what we obtain when we compute the partition function). It is worth mentioning, however, that for large N , such a computation becomes impracticable. For instance, for $N = 2, 3$, and 4 , the dimension of W is 16, 64, and 256, respectively.

The method just presented can also be used for numerical calculations. Even though the matrices become very large as N increases, they are extremely sparse. Using sparse matrix algorithms, we are able to simulate systems up to $N = 8$. It is worth mentioning that other methods, such as the time-evolving block decimation method [24], can reach much larger sizes. These methods, however, are asymptotically convergent, whereas the method described above is numerically exact.

V. EXACT SOLUTION FOR $N = 2$

The size $N = 2$ is an exception in that it presents no rectification. This is a feature of the present choice of Lindblad operators. For $N > 2$, the system always presents rectification

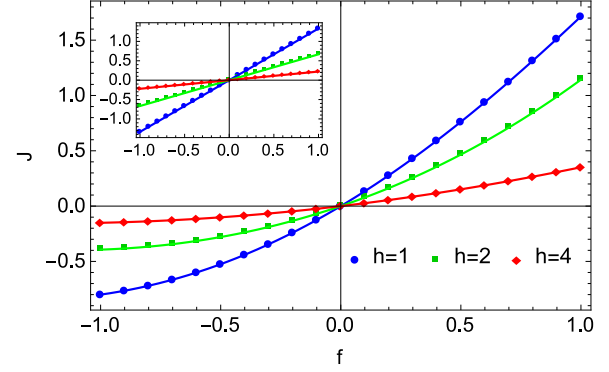


FIG. 1. (Color online) Flux J vs f for $N = 3$, $\Delta = 1$, and different values of h . The points correspond to simulations and the solid line corresponds to Eq. (34). Inset: Same but for $N = 2$ [cf. Eq. (33)].

as long as $\Delta \neq 0$. The steady-state density matrix ρ_{ss} was computed by solving Eq. (31). To write the result, let us define

$$a = \alpha^2 \gamma^2, \\ b = \gamma^2 (\gamma^2 + h^2).$$

Then the result for ρ_{ss} is

$$\rho_{ss} = \frac{1}{4(a+b)} \begin{pmatrix} \rho_{11} & 0 & 0 & 0 \\ 0 & \rho_{22} & \rho_{23} & 0 \\ 0 & \rho_{23}^* & \rho_{33} & 0 \\ 0 & 0 & 0 & \rho_{44} \end{pmatrix}, \quad (32)$$

where

$$\rho_{11} = b(1 - f^2) + a, \\ \rho_{22} = b(1 + f^2) + a, \\ \rho_{33} = b(1 - f)^2 + a, \\ \rho_{44} = b(1 - f^2) + a, \\ \rho_{23} = 2\alpha\gamma^2 f(h + i\gamma).$$

As can be seen, Δ has completely dropped out from this result. For this reason, when $N = 2$, there is no rectification.

The heat flux is computed from any one of Eqs. (9)–(11) and is proportional to the imaginary part of the off-diagonal element ρ_{23} . It reads

$$J = \frac{4f\alpha^2\gamma}{\alpha^2 + \gamma^2 + h^2}. \quad (33)$$

This result is illustrated in the inset of Fig. 1 as a function of f for different values of h and $\alpha = \gamma = 1$.

VI. EXACT SOLUTION FOR $N = 3$

When $N = 3$, the matrix W appearing in Eq. (31) has dimensions $2^{2 \times 3} = 64$. For simplicity, we now assume $\alpha = \gamma = 1$. The solution for the full density matrix is somewhat cumbersome so we shall only present the flux.

It reads

$$J(f) = 4f \frac{a_0 + 2a_1fh\Delta + a_2\Delta^2}{b_0 - 2b_1fh\Delta + b_2\Delta^2 + b_4\Delta^4}, \quad (34)$$

where the coefficients a_i and b_i are *even functions* of both f and h :

$$\begin{aligned} a_0 &= (2 + h^2)(12 + h^2), \\ a_1 &= 2 + h^2, \\ a_2 &= 4 + 3h^2 - 2f^2(1 + h^2), \\ b_0 &= (2 + h^2)^2(12 + h^2), \\ b_1 &= 8 + 9h^2, \\ b_2 &= 14 + 11h^2 - 2h^4 + 2f^2(1 + h^2), \\ b_4 &= 1 + h^2. \end{aligned}$$

When f is small, Eq. (34) simplifies to

$$J \simeq 4f \frac{a_0 + a_2\Delta^2}{b_0 + b_2\Delta^2 + b_4\Delta^4},$$

and, to first order in both f and h , this reduces further to

$$J \simeq \frac{16f}{8 + \Delta^2}.$$

$$R = 2fh\Delta \frac{(a_1b_0 + a_0b_1) + (a_1b_2 + a_2b_1)\Delta^2 + a_1b_4\Delta^4}{a_0b_0 + (a_0b_2 + a_2b_0 + 4a_1b_1f^2h^2)\Delta^2 + (a_2b_2 + a_0b_4)\Delta^4 + a_2b_4\Delta^6}. \quad (35)$$

This formula is quite interesting. Besides the factor of $2fh\Delta$, the rest of the expression is even in f , h , and Δ . Hence, R is an odd function in these three parameters and is zero if any of f , h , and Δ are zero. Equation (35) takes on a particularly simple form when we expand it to first order in both f and h :

$$R \simeq fh\Delta \frac{24 + \Delta^2}{(6 + \Delta^2)(8 + \Delta^2)}. \quad (36)$$

To first order in all three parameters, this reduces further to

$$R \simeq \frac{fh\Delta}{2}. \quad (37)$$

The rectification coefficient, given by Eq. (35), is plotted in Fig. 3 as a function of Δ for $f = 0.5$ and different values of h .

The symmetry embodied in Eq. (16) is evident in Figs. 2 and 3: the behavior of $J(f)$ for $\Delta < 0$ is the same as $J(-f)$ for $\Delta > 0$, which makes R an odd function of Δ . Hence, from now on, we will focus only on the case $\Delta > 0$.

VII. NUMERICAL SOLUTION

A. General behavior of larger sizes

In this section, we consider the numerical solution for sizes up to $N = 7$. In Fig. 4, we present J vs Δ for $f = 0.5$. When $\Delta = 0$, the flux is seen to be independent of the size. This situation corresponds to the XX model that will be discussed in Appendix C. When h is small, the solution is qualitatively similar for different sizes [Fig. 4(a)]. But for larger values of

The flux in Eq. (34) is depicted in Fig. 1 as a function of f for different values of h , together with the numerical simulations for comparison. Unlike the case $N = 2$, we now see that J is not an odd function of f , so this system will present rectification. Curves of the form shown in Fig. 1 are a signature of rectification and appear frequently in papers on this subject (cf. Ref. [13]). We emphasize, however, that the present solution is exact and not numerical, like in most cases.

Much more interesting is the dependence of the flux J on Δ . This is shown in Fig. 2. In Fig. 2(a), we show plots for $f = 0.5$. We see that J decreases rapidly with Δ in all cases. When $h = 0$, the flux behaves as a single symmetric peak centered around $\Delta = 0$. In this case, $J(-f) = -J(f)$ so there is no rectification. When we increase h , this peak is shifted toward positive Δ and a second, smaller peak appears at negative Δ . As we reduce f , the two peaks become increasingly more symmetric, as is evident in Fig. 2(b) where we plot the limit of J/f as $f \rightarrow 0$. Finally, in the opposite limit where $f = 1$, only one peak survives. Note that as long as $h \neq 0$ and $\Delta \neq 0$, there is rectification since $J(-f) \neq -J(f)$.

The rectification coefficient may be computed by inserting Eq. (34) in Eq. (14). The result is

h , different patterns are observed. A similar behavior occurs for the rectification coefficient plotted in Fig. 5.

B. Solution for small f , h , and Δ

We now discuss the behavior of R when f , h , and Δ are small, with fixed $\alpha = \gamma = 1$. For $N = 3$, we obtained the linear behavior in Eq. (37). Since R must be odd in all three parameters, it is reasonable to suppose that to first order in f , h , and Δ ,

$$R = A_N fh\Delta, \quad (38)$$

where the prefactor A_N depends on the size N , and also on α and γ , whose dependences we are omitting (we mention, nonetheless, that $A_N = 0$ trivially if either α or γ are zero). The numerical results for A_N when $\alpha = \gamma = 1$ are shown in Fig. 6. We see that it increases with N , tending to a finite value. This is a very important result since it indicates that R should remain finite in the thermodynamic limit $N \rightarrow \infty$.

From the discussion in Sec. IV, we have found that R must always be a ratio of polynomials in f , h , and Δ . Also, the master equation (2) contains only whole numbers multiplying the parameters. Hence, A_N must be a rational number for each size N (and for $\alpha = \gamma = 1$). To determine the A_N , we performed the simulations in Fig. 6 using arbitrary precision arithmetic so that they could be rationalized. The sequence of numbers so obtained for $N = 3$ through 8 was $\frac{1}{2}$, $\frac{5}{6}$, 1 , $\frac{11}{10}$, $\frac{7}{6}$, and $\frac{17}{14}$. From this, we can formulate the ansatz,

$$A_N = \frac{3}{2} - \frac{2}{N-1}, \quad (39)$$

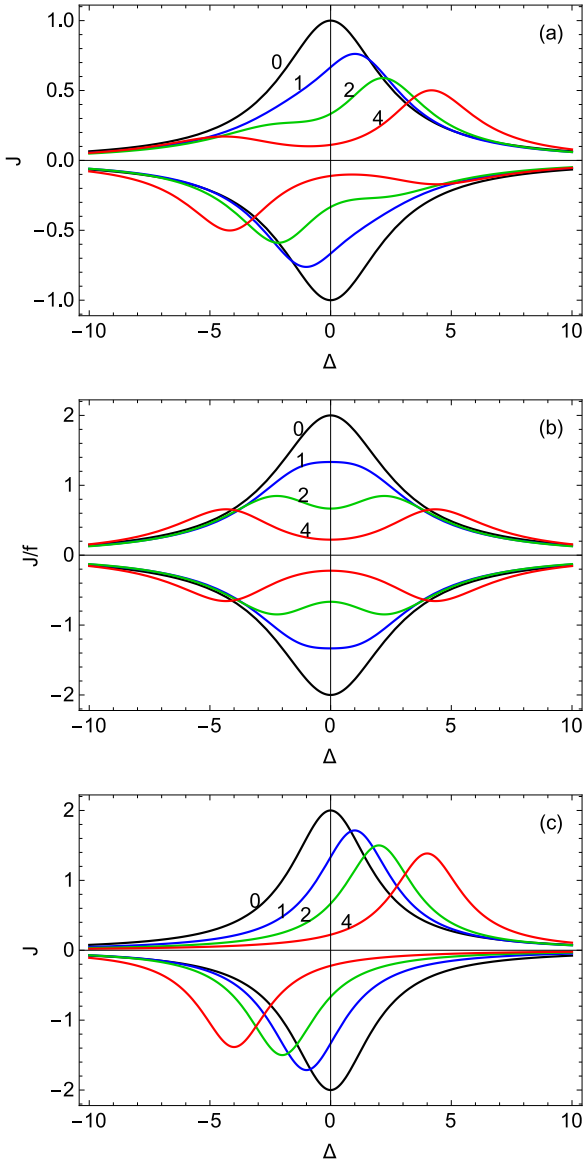


FIG. 2. (Color online) $J(f)$ (upper curves) and $J(-f)$ (lower curves) vs Δ for $N = 3$ and $h = 0, 1, 2,$ and 4 (as signaled in each figure). (a) $f = 0.5$, (b) $f \rightarrow 0$, and (c) $f = 1$. In (b), we plot the limit of J/f as $f \rightarrow 0$.

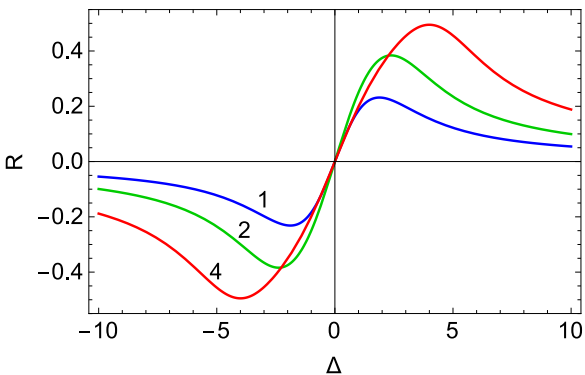


FIG. 3. (Color online) Rectification coefficient R vs Δ for $N = 3$, $f = 0.5$, and different values of h , as signaled in the figure. See Eq. (35).

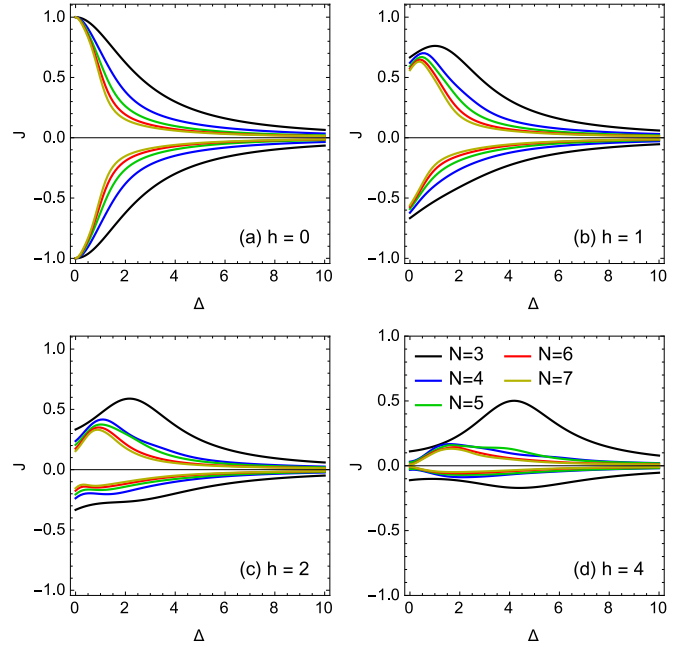


FIG. 4. (Color online) $J(f)$ (upper curve) and $J(-f)$ (lower curve) vs Δ for $f = 0.5$, different values of h (as shown in the label of each image), and different sizes [as shown in image (d)].

which is valid for $N \geq 3$. Hence, to first order in f , h , and Δ , we conjecture that the rectification for any size N is given by

$$R \simeq \left[\frac{3}{2} - \frac{2}{N-1} \right] fh\Delta.$$

Taking $N \rightarrow \infty$ then gives (again to first order)

$$R \simeq \frac{3}{2} fh\Delta, \tag{40}$$

from which it follows that, indeed, in the thermodynamic limit, the rectification coefficient remains finite.

C. Solution for small f and h , but arbitrary Δ

Next let us investigate the rectification when f and h are both small, but Δ is not necessarily so. When $N = 3$, we obtained the behavior shown in Eq. (36). The results for other sizes are shown in Fig. 7. We know that the rectification is always a ratio of polynomials in all parameters. Hence, if

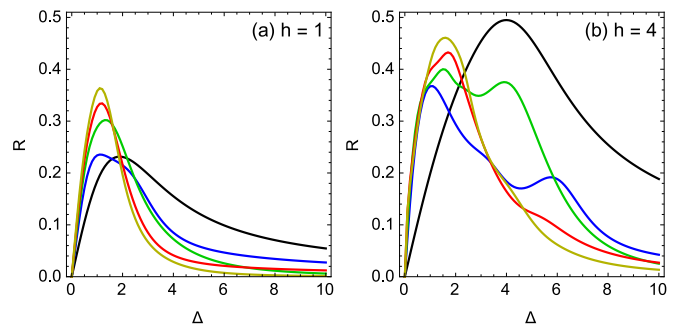


FIG. 5. (Color online) R vs Δ for $f = 0.5$, different values of h (as shown in the label of each image), and different sizes. The color scheme is the same as Fig. 4.

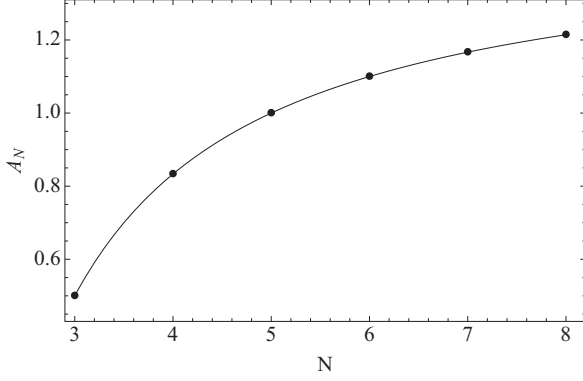


FIG. 6. The function $A_N = R/fh\Delta$ for different values of N , as obtained from arbitrary precision simulations. The solid line corresponds to Eq. (39).

we expand to first order in f and h , we always expect to obtain R in the form $R \simeq fhq_1(\Delta)/q_2(\Delta)$, where q_1 and q_2 are polynomials in Δ . The order of these polynomials increases with N , but we may look for a lower order Padé approximant. From the numerical simulations, we have found that for $N = 3$ to 7, the results are all very well described by

$$R \simeq A_N fh\Delta \frac{1 + v_1 \Delta^2}{1 + v_2 \Delta^2 + v_3 \Delta^4}, \quad (41)$$

where v_1 , v_2 , and v_3 are fit parameters that depend on N . This is the (3,4) Padé approximant of the actual solution. This same idea can be used to study R in other cases; for instance, when f and Δ are small, but h is not.

VIII. ABSENCE OF RECTIFICATION WHEN $\Delta = 0$

As we have discussed, the rectification coefficient R is zero when $f = 0$, since this means there is no flux from one bath to the other. Moreover, $R = 0$ when $h = 0$ since this means the system is symmetric (recall that by h , we mean the linear field gradient which ranges from $-h$ to h). However, we have also seen that $R = 0$ when $\Delta = 0$, a result which does not bear the same physical intuition of the above. In this section, we wish

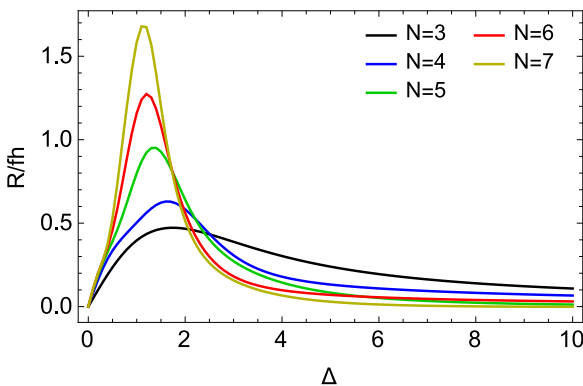


FIG. 7. (Color online) The rectification coefficient R/fh vs Δ for $f = 0.01$, $h = 0.01$, and different values of N , as denoted in the figure.

to prove that $R(\Delta = 0) = 0$. An alternative proof, based on the covariance matrix, is discussed in Appendix C.

Our goal is to prove Eq. (16), from which our result follows immediately. To accomplish this, we shall investigate three symmetry operations performed on the steady-state solution of Eq. (5), which we rewrite more explicitly as

$$\mathcal{W}(\alpha, \Delta, h, f)(\rho) = 0.$$

The solution of this equation is $\rho(\alpha, \Delta, h, f)$ (for simplicity, in this section we write the solution as ρ instead of ρ_{ss}).

The first symmetry is based on the following unitary transformation:

$$U = \prod_{i=1,3,5,\dots} \sigma_i^z.$$

It maps

$$UH(\alpha, \Delta, h_i)U^\dagger = H(-\alpha, \Delta, h_i)$$

and

$$UD(\rho)U^\dagger = D(U\rho U^\dagger).$$

Hence,

$$U\{\mathcal{W}(\alpha, \Delta, h, f)(\rho)\}U^\dagger = \mathcal{W}(-\alpha, \Delta, h, f)(U\rho U^\dagger) = 0.$$

But this is the equation which gives the solution $\rho(-\alpha, \Delta, h, f)$. Hence, we conclude that

$$\rho(-\alpha, \Delta, h, f) = U\rho(\alpha, \Delta, h, f)U^\dagger. \quad (42)$$

That is, the two density matrices are similar (share the same eigenvalues).

Next consider the flux, as computed from Eq. (9), and define $\mathcal{J}(\alpha) = 2\alpha(\sigma_i^x \sigma_{i+1}^y - \sigma_i^y \sigma_{i+1}^x)$. Then, by definition,

$$J(\alpha, \Delta, h, f) = \text{tr}[\mathcal{J}(\alpha)\rho(\alpha, \Delta, h, f)] \quad (43)$$

and

$$\begin{aligned} J(-\alpha, \Delta, h, f) &= \text{tr}[\mathcal{J}(-\alpha)\rho(-\alpha, \Delta, h, f)] \\ &= \text{tr}[\mathcal{J}(-\alpha)U\rho(\alpha, \Delta, h, f)U^\dagger]. \end{aligned}$$

Using that $U^\dagger \mathcal{J}(\alpha)U = \mathcal{J}(-\alpha)$ then yields

$$J(-\alpha, \Delta, h, f) = J(\alpha, \Delta, h, f).$$

Hence, the flux is invariant by a reversal of α .

Next, consider the transformation

$$V = \prod_{i=1}^N \sigma_i^x.$$

It maps

$$VH(\alpha, \Delta, h)V^\dagger = H(\alpha, \Delta, -h)$$

and

$$VD(\rho, f)V^\dagger = D(V\rho V^\dagger, -f).$$

Hence,

$$V[\mathcal{W}(\alpha, \Delta, h, f)(\rho)]V^\dagger = \mathcal{W}(\alpha, \Delta, -h, -f)(V\rho V^\dagger).$$

Therefore, the density matrices are related via

$$\rho(\alpha, \Delta, -h, -f) = V\rho(\alpha, \Delta, h, f)V^\dagger. \quad (44)$$

If we also use the fact that $V\mathcal{J}(\alpha)V^\dagger = -\mathcal{J}(\alpha)$, we obtain

$$J(\alpha, \Delta, h, f) = -J(\alpha, \Delta, -h, -f).$$

This transformation has an intuitive physical interpretation. It shows that if we simultaneously reverse the baths and the flux gradient, we obtain a similar density matrix and a flux that is simply of the opposite sign.

Finally, let us consider the operation of complex conjugation [31,32], assuming we are working with the usual basis (where σ_i^z is diagonal). We have

$$\begin{aligned} \{-i[H(\alpha, \Delta, h), \rho]\}^* &= -i[H(-\alpha, -\Delta, -h), \rho^*], \\ \{D(\rho)\}^* &= D(\rho^*). \end{aligned}$$

Hence,

$$\{\mathcal{W}(\alpha, \Delta, h, f)(\rho)\}^* = \mathcal{W}(-\alpha, -\Delta, -h, f)(\rho^*).$$

But the solution of this last equation is $\rho(-\alpha, -\Delta, -h, f)$ so we conclude that

$$\rho^*(\alpha, \Delta, h, f) = \rho(-\alpha, -\Delta, -h, f). \quad (45)$$

Combining the three symmetry operations summarized by Eqs. (42), (44), and (45), we obtain

$$VU\rho(\alpha, \Delta, h, f)U^\dagger V^\dagger = \rho^*(\alpha, -\Delta, h, -f). \quad (46)$$

Applying this result in Eq. (43) yields Eq. (16), thus completing the proof.

IX. CONCLUSIONS

The goal of this paper was to study rectification in a system which could, at least to some extent, be treated analytically. The system of choice was the XXZ chain under two Lindblad baths. We studied the flux J and the rectification coefficient R both exactly and numerically, which enabled us to extract several important properties of the rectification. In particular, we have emphasized the functional dependence of R on the three main parameters of the model: the driving strength (bath difference) f , the field gradient h (that makes the system asymmetric), and the anisotropy parameter Δ . We have shown that R is odd in all three of them, thus being zero when any one is zero. This shows that they correspond to the three necessary ingredients for the existence of rectification. We have also shown that to first order in f , h , and Δ , the rectification behaves as $R = A_N f h \Delta$. The coefficient A_N was determined by combining numerical simulations with exact calculations. In particular, when $N \rightarrow \infty$, we found that $A_N \rightarrow 3/2$. This shows that the rectification is finite in the thermodynamic limit, a most relevant result. Finally, the fact that $R(\Delta = 0) = 0$ was proven using symmetries of the Lindblad master equation.

ACKNOWLEDGMENTS

The authors would like to acknowledge the Brazilian funding agency FAPESP for the financial support. We also thank one of the reviewers of the paper for pointing out the complex conjugation operation used in Sec. VIII.

APPENDIX A: THE REPEATED INTERACTIONS SCHEME

In this Appendix, we discuss the repeated interaction scheme [33], which is a discrete version of the master equation (2). From this scheme, it is then possible to derive Eq. (2) as an appropriate limit, as shown in Appendix B.

The idea of the repeated interactions scheme is as follows. First we augment our spin chain with two additional spins, labeled 0 and $N + 1$. These spins are coupled to the spins 1 and N , respectively, and, for simplicity, we assume that this coupling has $\Delta = 0$. Hence the total Hamiltonian of our augmented system is

$$H_T = H + h_0\sigma_0^z + h_{N+1}\sigma_{N+1}^z + V_0 + V_N, \quad (A1)$$

where H is our original Hamiltonian [Eq. (1)] and $V_i = \alpha(\sigma_i^x\sigma_{i+1}^x + \sigma_i^y\sigma_{i+1}^y)$ describes the interaction between spins 0 and 1, and spins N and $N + 1$.

We now assume that at $t = 0$, the system is decoupled from the spins 0 and $N + 1$ so that the total density matrix ρ_T may be factored as a product,

$$\rho_T(0) = \rho_L\rho(0)\rho_R, \quad (A2)$$

where ρ_L and ρ_R are the density matrices of spins 0 and $N + 1$, respectively. Further, we assume that at $t = 0$, these two spins are in thermal equilibrium so we may write

$$\rho_L = \frac{(1 + f_L)}{2}|z_+\rangle\langle z_+| + \frac{(1 - f_L)}{2}|z_-\rangle\langle z_-|, \quad (A3)$$

where $f_L = \tanh(\beta_0 h_0)$ and β_0 is the inverse temperature of the left spin. A similar formula holds for ρ_R ,

$$\rho_R = \frac{(1 + f_R)}{2}|z_+\rangle\langle z_+| + \frac{(1 - f_R)}{2}|z_-\rangle\langle z_-|, \quad (A4)$$

where $f_R = \tanh(\beta_{N+1} h_{N+1})$. Note that $f_L = \langle\sigma_0^z\rangle$ and $f_R = \langle\sigma_{N+1}^z\rangle$, which gives a clear physical interpretation of the parameters f_L and f_R .

The dynamics of the augmented system is now described by the standard Von Neumann equation,

$$\frac{d\rho_T}{dt} = -i[H_T, \rho_T],$$

whose formal solution is

$$\rho_T(t) = U(t)\rho_T(0)U^\dagger(t),$$

with $U(t) = e^{-iH_T t}$ being the time propagator.

We now arrive at the *repeated interactions scheme*. We start at $t = 0$ with $\rho_T(0)$ factored as in Eq. (A2) and allow the system to evolve up to a time τ , at which

$$\rho_T(\tau) = U(\tau)[\rho_L\rho(0)\rho_R]U^\dagger(\tau).$$

Then, at $t = \tau$, we “throw away” the spins 0 and $N + 1$ and get fresh new ones from a thermal bath. Thus, we first obtain $\rho(\tau)$ by taking the partial trace over the spins 0 and $N + 1$,

$$\rho(\tau) = \text{tr}_{L,R}[\rho_T(\tau)],$$

and then we construct

$$\rho_T(\tau) = \rho_L\rho(\tau)\rho_R,$$

where ρ_L and ρ_R are again given by Eqs. (A3) and (A4). We then repeat this process up to time 2τ , when we again throw

away the boundary spins and get fresh new ones, and so on. This idea is based on Boltzmann's Stosszahlansatz.

If we let $\rho_n = \rho(n\tau)$ be the density matrix of the (reduced) system at time $t = n\tau$, then this entire procedure can be summarized by

$$\rho_{n+1} = \text{tr}_{L,R}[U(\tau)(\rho_L \rho_n \rho_R)U^\dagger(\tau)]. \quad (\text{A5})$$

This is a discrete mapping for the time evolution of $\rho(t)$ and can be seen as the quantum version of a Markov chain. This mapping will eventually reach a steady state ρ_{ss} defined by

$$\rho_{\text{ss}} = \text{tr}_{L,R}[U(\tau)(\rho_L \rho^* \rho_R)U^\dagger(\tau)].$$

It is perfectly possible to use this framework to study the dynamics of the system. The only additional parameter is the time of interaction τ . However, it is more convenient to study the limit $\tau \rightarrow 0$, which will lead us to the Lindblad equation used in this paper.

APPENDIX B: FROM REPEATED INTERACTIONS TO LINDBLAD

We now show how to derive the master equation (2) from the discrete mapping in Eq. (A5). For this, we may use the Baker-Campbell-Hausdorff formula to write

$$e^{-iH_T\tau} \rho_T e^{iH_T\tau} = \rho_T - i\tau[H_T, \rho_T] - \frac{\tau^2}{2}[H_T, [H_T, \rho_T]] + \dots$$

We then insert this into Eq. (A5) and take the partial traces. The first term gives $\text{tr}_{L,R}(\rho_L \rho_n \rho_R) = \rho_n$. As for the second term, it can be verified that

$$\text{tr}_{L,R}\{[H_T, \rho_T]\} = [H, \rho_n].$$

Note, however, that this is not necessarily true for all Hamiltonians. It is, in our case, due to our choice of V_i in Eq. (A1).

Thus we see that to first order in τ , the coupling to the boundary spins becomes negligible. This is physically intuitive: if the interaction time τ goes to zero, then so does the interaction. In order to obtain a finite contribution, we must therefore also let V_i increase with τ . The correct way to do this, in order to obtain a finite limit, is to let V_i increase as

$$V_i = \sqrt{\frac{\gamma}{\tau}}(\sigma_i^x \sigma_{i+1}^x + \sigma_i^y \sigma_{i+1}^y),$$

where γ is a new constant. This is similar to what happens in the Langevin solution of classical Brownian motion: if we make the noise infinitesimally short, then we must also make it infinitely large in order to give a non-negligible contribution. Hence, define

$$-\frac{\tau^2}{2}[V_0, [V_0, \rho_T]] := \tau D_L(\rho),$$

$$-\frac{\tau^2}{2}[V_N, [V_N, \rho_T]] := \tau D_R(\rho).$$

After going through the algebra, one obtains the formulas appearing in Eq. (4). Equation (A5) thus becomes

$$\rho_{n+1} = \rho_n - i\tau[H, \rho_n] + \tau[D_L(\rho_n) + D_R(\rho_n)].$$

Finally, dividing by τ and taking the limit $\tau \rightarrow 0$ produces the master equation (2).

APPENDIX C: EXACT SOLUTION OF THE XX CHAIN

In this section, we study the exact solution in the case when $\Delta = 0$ in Eq. (1), which is nothing but the XX model. This analysis will also give an alternative way of seeing that the rectification is zero when $\Delta = 0$.

The XX chain may be treated exactly using fermionic operators [34],

$$c_k = \left[\prod_{j=1}^{k-1} e^{i\pi\sigma_k^+ \sigma_j^-} \right] \sigma_k^- \quad (\text{C1})$$

and c_k^\dagger . These operators satisfy $\{c_k, c_\ell^\dagger\} = \delta_{k,\ell}$. In terms of them, Eq. (1) (with $\Delta = 0$) becomes

$$H = \sum_{i=1}^N 2h_i c_i^\dagger c_i + 2\alpha \sum_{i=1}^{N-1} (c_i^\dagger c_{i+1} + c_{i+1}^\dagger c_i).$$

Instead of solving for the density matrix, in this case we can obtain a closed system of equations for the covariance matrix,

$$C_{k,\ell} = \langle c_k^\dagger c_\ell \rangle = \text{tr}(c_k^\dagger c_\ell \rho). \quad (\text{C2})$$

This suffices for our purposes since J in Eq. (9) is entirely determined by the entries of C :

$$J = 4i\alpha(C_{k,k+1} - C_{k+1,k}). \quad (\text{C3})$$

Using the master equation (2) with Eq. (C2), it is possible to obtain the following system of linear equations for C :

$$\frac{dC}{dt} = AC + CA^\dagger - F, \quad (\text{C4})$$

where

$$A_{k,\ell} = 2i[h_\ell \delta_{k,\ell} + \alpha \delta_{k+1,\ell} + \alpha \delta_{k-1,\ell}] - 2\gamma[\delta_{k,1} \delta_{\ell,1} + \delta_{k,N} \delta_{\ell,N}], \quad (\text{C5})$$

$$F_{k,\ell} = -2\gamma[(1 + f_L)\delta_{k,1} \delta_{\ell,1} + (1 + f_R)\delta_{k,N} \delta_{\ell,N}]. \quad (\text{C6})$$

Note that we are assuming a general field distribution h_ℓ . The steady-state solution is then obtained by setting $dC/dt = 0$ in Eq. (C4), leading to the Lyapunov equation [35],

$$AC + CA^\dagger = F. \quad (\text{C7})$$

Since, by construction, C is Hermitian, we may write $CA^\dagger = (AC)^\dagger$. Thus, Eq. (C7) says that the Hermitian part of AC should be proportional to F , whereas the anti-Hermitian part should be zero.

The arguments that follow will be valid for any f_L and f_R . Hence let us parametrize them as $f_L = f_0 + f$ and $f_R = f_0 - f$ (thus far in the paper we have been using $f_0 = 0$). We may then write Eq. (C6) as

$$F = -2\gamma[(1 + f_0)\Theta + f\Upsilon], \quad (\text{C8})$$

where

$$\Theta = \text{diag}(1,0,0, \dots, 0,0,1), \quad (\text{C9})$$

$$\Upsilon = \text{diag}(1,0,0, \dots, 0,0, -1). \quad (\text{C10})$$

Moreover, the matrix A in Eq. (C5) can be written as

$$A = -2\gamma(\Theta - iT), \quad (\text{C11})$$

where

$$T_{k,\ell} = t_\ell \delta_{k,\ell} + \beta(\delta_{k+1,\ell} + \delta_{k-1,\ell}), \quad (\text{C12})$$

and where we have defined the rescaled parameters $t_\ell = h_\ell/\gamma$ and $\beta = \alpha/\gamma$. These definitions make it clear that the covariance matrix will depend only on the parameters t_ℓ , β , f_0 , and f .

With these definitions in hand, we may divide Eq. (C7) by -2γ and write it as

$$\{\Theta, C\} - i[T, C] = (1 + f_0)\Theta + f\Upsilon. \quad (\text{C13})$$

Let C^0 be the solution of Eq. (C13) when $f = 0$, i.e.,

$$\{\Theta, C^0\} - i[T, C^0] = (1 + f_0)\Theta. \quad (\text{C14})$$

It can be verified by direct substitution that

$$C^0 = \frac{1}{2}(1 + f_0)I, \quad (\text{C15})$$

where I is the identity matrix of dimension N . Let us then define

$$C = C^0 + fC^I.$$

Inserting this into Eq. (C13) and using Eq. (C14) yields the following equation for C^I :

$$\{\Theta, C^I\} - i[T, C^I] = \Upsilon. \quad (\text{C16})$$

This equation is *independent* of f . This, in a sense, suffices to show that the rectification is always zero in the XX model: since C^0 is diagonal, the flux (C3) will depend only on C^I through

$$J = 4i\alpha f [C^I_{i,i+1} - C^I_{i+1,i}].$$

By reversing the baths (i.e., by making $f \rightarrow -f$), we thus see that $J(-f) = -J(f)$. Hence the rectification coefficient, as defined in Eq. (14), is zero.

The similarity with the classical case is worth noting [36]. As here, when the forces are harmonic, it is possible to obtain a closed system of equation for the covariances, from which the flux is determined to be linear in the bath difference f . Conversely, when anharmonic terms (higher than quadratic) appear in the Hamiltonian, the equations are no longer closed; that is, the equation for the covariances would depend on higher order correlations.

To finish, let us also present the solution of Eq. (C16) for certain field distributions. First we write

$$C^I = X + iY$$

for real matrices X and Y . Since $C^\dagger = C$, we have that $X^T = X$ and $Y^T = -Y$. Inserting this in Eq. (C16) yields the following real equations for X and Y :

$$[T, X] - \{\Theta, Y\} = 0, \quad (\text{C17})$$

$$[T, Y] + \{\Theta, X\} = \Upsilon. \quad (\text{C18})$$

When all $h_i = h$, the field terms completely drop out of Eqs. (C17) and (C18). In this case, the solution is

$$X = \frac{1}{2} \frac{1}{\beta^2 + 1} \Upsilon,$$

$$Y = -\frac{1}{2} \frac{\beta}{\beta^2 + 1} S^y,$$

where $(S^y)_{k,\ell} = \delta_{k+1,\ell} - \delta_{k-1,\ell}$.

Another interesting situation is when $h_1 = -h$, $h_N = h$, and all other $h_i = 0$ (note that this is different from the linear field gradient we have been using so far). In this case, the solution is

$$X = \frac{1}{2} \frac{1}{\beta^2 + t^2 + 1} [(t^2 + 1)\Upsilon - \beta t S^x],$$

$$Y = -\frac{1}{2} \frac{\beta}{\beta^2 + t^2 + 1} S^y,$$

where $(S^x)_{k,\ell} = \delta_{k+1,\ell} + \delta_{k-1,\ell}$ and $t = h/\gamma$. The important point to be noticed here is that the steady-state covariances are size independent and tridiagonal. This means that the correlations are strictly local, being reduced to the occupation density C_{kk} and the nearest neighbor correlation $C_{k,k+1}$. Remarkably this is true only in this particular case. For other field distributions, the correlations $C_{k,\ell}$ are nonzero for any (k, ℓ) .

-
- [1] W. H. Brattain, *Rev. Mod. Phys.* **23**, 203 (1951).
 [2] C. Starr, *J. Appl. Phys.* **7**, 15 (1936).
 [3] E. Nefzaoui, K. Joulain, J. Drevillon, and Y. Ezzahri, *Appl. Phys. Lett.* **104**, 103905 (2014).
 [4] N. Yang, G. Zhang, and B. Li, *Appl. Phys. Lett.* **95**, 033107 (2009).
 [5] J. Hu, X. Ruan, and Y. P. Chen, *Nano Lett.* **9**, 2730 (2009).
 [6] W. Kobayashi, Y. Teraoka, and I. Terasaki, *Appl. Phys. Lett.* **95**, 171905 (2009).
 [7] R. Scheibner, M. König, D. Reuter, A. D. Wieck, C. Gould, H. Buhmann, and L. W. Molenkamp, *New J. Phys.* **10**, 083016 (2008).
 [8] C. W. Chang, D. Okawa, A. Majumdar, and A. Zettl, *Science* **314**, 1121 (2006).
 [9] Y. Yan, C.-Q. Wu, and B. Li, *Phys. Rev. B* **79**, 014207 (2009).
 [10] L. Zhang, Y. Yan, C.-Q. Wu, J.-S. Wang, and B. Li, *Phys. Rev. B* **80**, 172301 (2009).
 [11] R. R. Ávila and E. Pereira, *J. Phys. A* **46**, 055002 (2013).
 [12] M. Romero-Bastida and J. M. Arizmendi-Carvajal, *J. Phys. A* **46**, 115006 (2013).
 [13] B. Li, L. Wang, and G. Casati, *Phys. Rev. Lett.* **93**, 184301 (2004); B. Li, J. H. Lan, and L. Wang, *ibid.* **95**, 104302 (2005); B. Hu, L. Yang, and Y. Zhang, *ibid.* **97**, 124302 (2006).
 [14] L. Wang and B. Li, *Phys. Rev. Lett.* **99**, 177208 (2007).

- [15] W. C. Lo, L. Wang, and B. Li, *J. Phys. Soc. Japan* **77**, 054402 (2008).
- [16] N. Li, J. Ren, L. Wang, G. Zhang, P. Hänggi, and B. Li, *Rev. Mod. Phys.* **84**, 1045 (2012).
- [17] N. Roberts and D. Walker, *Intl. J. Thermal Sci.* **50**, 648 (2011).
- [18] E. Pereira, *Phys. Rev. E* **83**, 031106 (2011).
- [19] Z. Rieder, J. L. Lebowitz, and E. Lieb, *J. Math. Phys.* **8**, 1073 (1967).
- [20] H.-P. Breuer and F. Petruccione, *The Theory of Open Quantum Systems* (Oxford University Press, New York, 2002), p. 636.
- [21] D. Karevski, V. Popkov, and G. M. Schütz, *Phys. Rev. Lett.* **110**, 047201 (2013).
- [22] T. Prosen, *Phys. Rev. Lett.* **106**, 217206 (2011).
- [23] T. Prosen, *Phys. Rev. Lett.* **107**, 137201 (2011).
- [24] J. J. Mendoza-Arenas, S. Al-Assam, S. R. Clark, and D. Jaksch, *J. Stat. Mech.* (2013) P07007.
- [25] V. Popkov, D. Karevski, and G. M. Schütz, *Phys. Rev. E* **88**, 062118 (2013).
- [26] T. Platini, R. J. Harris, and D. Karevski, *J. Phys. A* **43**, 135003 (2010).
- [27] V. V. Albert and L. Jiang, *Phys. Rev. A* **89**, 022118 (2014).
- [28] T. Prosen, *Physica Scripta* **86**, 058511 (2012).
- [29] D. Evans, *Commun. Math. Phys.* **54**, 293 (1977).
- [30] N. G. van Kampen, *Stochastic Processes in Physics and Chemistry* (North-Holland, Amsterdam, 2007).
- [31] V. Popkov and R. Livi, *New J. Phys.* **15**, 023030 (2013).
- [32] V. Popkov, *J. Stat. Mech.* (2012) P12015.
- [33] D. Karevski and T. Platini, *Phys. Rev. Lett.* **102**, 207207 (2009).
- [34] E. Lieb, T. Schultz, and D. Mattis, *Rev. Mod. Phys.* **36**, 856 (1964).
- [35] R. Bartels and G. Stewart, *Commun. ACM* **15**, 820 (1972).
- [36] G. T. Landi and M. J. de Oliveira, *Phys. Rev. E* **89**, 022105 (2014).